Astronomy & Astrophysics manuscript no. February 1, 2008
(DOI: will be inserted by hand later)

A superburst from GX 3+1

Erik Kuulkers[1,2]

[1] SRON National Institute for Space Research, Sorbonnelaan 2, 3584 CA Utrecht, The Netherlands
[2] Astronomical Institute, Utrecht University, P.O. Box 80000, 3508 TA Utrecht, The Netherlands

Received –; accepted –

Abstract. I found one long X-ray flare from the X-ray burster GX 3+1 in almost 6 years of observations with the RXTE All Sky Monitor (ASM). The event had a peak flux of about 1.1 Crab (1.5-12 keV), lasted between 4.4 and 16.2 hours and exhibited a fluence of more than about 5×10^{41} erg for a source distance of 5 kpc. During the exponential-like decay, with an exponential decay time of 1.6 hours, spectral softening is seen. The total ASM effective exposure time on GX 3+1 is estimated to be around a year. The flare bears all the characteristics of the recently discovered so-called superbursts in other X-ray burst sources.

Key words. accretion, accretion disks — binaries: close — stars: individual (GX 3+1) — stars: neutron — X-rays: bursts

1. Introduction

Recently, six long X-ray flares lasting several hours have been identified in five low-mass X-ray binaries (Cornelisse et al. 2000, 2001, Strohmayer & Brown 2001; Wijnands 2001; Kuulkers et al. 2001). For one source, 4U 1636−53, two such events were reported which occurred about 4.7 years after each other (Wijnands 2001). So far, these flares have only been seen in X-ray bursters with persistent pre-flare luminosities of $\simeq$0.1–0.3 times the Eddington luminosity (Wijnands 2001; Kuulkers et al. 2001).

The long X-ray flares share many of the characteristics of type I X-ray bursts[1] and are, therefore, attributed to thermonuclear runaway events on a neutron star (e.g. Cornelisse et al. 2000). The differences with type I bursts are their long duration (exponential decay times of a few hours), their large fluences (about 10^{42} erg), and their rarity. Because of the large fluences, the flares are referred to as 'superbursts'. A likely fuel for the superbursts is carbon, left over from stable and unstable hydrogen and/or helium burning (Cumming & Bildsten 2001; Strohmayer & Brown 2001). Unstable electron capture by protons with subsequent capture of the resulting neutrons by heavy nuclei is another conceivable option (Kuulkers et al. 2001).

I here report on a superburst seen with the *Rossi X-ray Timing Explorer* (RXTE) All Sky Monitor (ASM) from GX 3+1 in June 1998. For a preliminary announcement of this event see Kuulkers (2001). The overall X-ray intensity of the GX 3+1 varies slowly on time scales of months to years by a factor of about 2 (e.g. Makishima et al. 1983; see Fig. 1a). Type I X-ray bursts in GX 3+1 were first discovered by Hakucho (Makishima et al. 1983). A type I X-ray burst with radius expansion (due to the burst luminosity reaching the Eddington limit) was observed by the Proportional Counter Array (PCA) onboard RXTE, enabling one to estimate the distance to the source to be in the range 4–6 kpc (Kuulkers & van der Klis 2000).

2. Observations and Analysis

The ASM (Levine et al. 1996) is one of the three instruments onboard RXTE. It consists of three Scanning Shadow Cameras (SSCs) mounted on a rotating drive such that the center of the field of view of one camera is perpendicular to that of the other two. The cameras are held stationary for 90-s intervals, called 'dwells', during which data are accumulated. The mount rotates the assembly through a 6° angle between dwells until a full rewind is necessary. In this manner about 80% of the sky is observed every 90-min orbit around the earth. Each dwell provides intensities in the 1.5–12 keV band for all known sources in the field of view of each camera, and results that meet a set of reliability criteria are saved in electronic tables that are available over the World Wide Web.

The ASM data are also available in three subbands: 1.5–3 keV, 3–5 keV, and 5–12 keV. The boundaries are, however, crude approximations. The actual channel boundaries change somewhat with time, anode, soft-

[1] Type I X-ray bursts have light curves with a rise which is faster than the exponential-like decay; their emission is well described by black-body radiation with temperatures, kT, around 2 keV and apparent black-body radii around 10 km; they show X-ray spectral softening during the decay. They have durations of seconds to minutes. For a review, see Lewin et al. (1993).

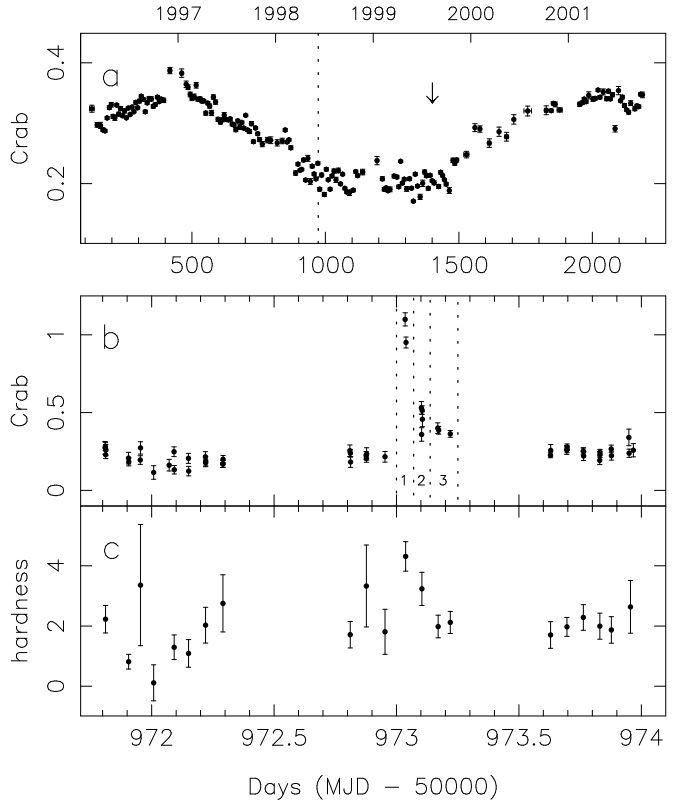

Fig. 1. **a)** RXTE/ASM (1.5–12 keV) light curve of GX 3+1 from 1996 (MJD 50088) to 2002 (MJD 52206). The data shown represent the mean of 7 consecutive daily averages and are normalized to the Crab count rate (75 cts s^{-1} SSC^{-1}). With a dotted line the time of the X-ray flare is shown. The time of the radius-expansion type I X-ray burst observed with the RXTE/PCA (Kuulkers & van der Klis 2000) is indicated by an arrow. **b)** Light curve of the individual RXTE/ASM dwells (normalised to Crab units; 1.5–12 keV) around the time of the flare. The dotted lines mark the three intervals used in the spectral analysis, see text. **c)** Hardness curve around the time of the flare. Hardness is defined as the ratio of the count rates in the 5–12 keV and 1.5–3 keV energy bands. Shown are averages of data which were less than 30 min apart, see text.

ware changes, etcetera. Moreover, the amount of these changes differ between the three SSCs (A. Levine 2001, priv. comm.). A pre-flight instrument effective area matrix for a source at the center of the field of view of an SSC is available, providing the detector response between 1 and 20 keV on an energy grid with a resolution of 0.1 keV[2]. It was used for estimating data system properties and rough sensitivities during the ASM development stage, and was certainly not designed for doing X-ray spectral fits to actual observations in three energy bands. There were small changes in the instrument design after the matrix numbers were computed, but the numbers were never updated (A. Levine 2001, priv. comm.). However, the matrix can be still useful for rough calculations, as done here. Note that a simple spectral model such as a black-body with only two free parameters may still be constrained by data in three energy bands.

The Crab (pulsar and nebula) is one of the main bright and steady X-ray calibration sources. Its observed ASM count rate is about 75 cts s^{-1} SSC^{-1} (1.5–12 keV, when at the center of an SSC field of view; see e.g. Levine et al. 1996). The pre-flight instrument effective area matrix, however, predicts a Crab count rate of about 88 cts s^{-1} SSC^{-1} in the same energy band. (The Crab spectrum in the energy band of interest can be described by an absorbed power-law; for the parameter values see e.g. Schattenburg & Canizares (1986), and references therein.) For doing X-ray spectral analysis one, therefore, has to renormalize the source count rates. The observed source count rates in a certain energy band were multiplied by the ratio of the predicted Crab count rate and the average observed Crab count rate in the same energy band. The latter were determined from the individual dwells during an interval centered around the observations, i.e MJD 50900–51050 (1998 March 28 to August 25). The resulting source count rates were then input for my spectral fitting. The rms in the average Crab count rates was included in the uncertainties of the source count rates (4.5%, 13%, 5% and 5%, in the 1.5–12 keV, 1.5–3 keV, 3–5 keV and 5–12 keV bands, respectively). Note that the errors in the individual dwell measurements contain already, apart from counting statistics, a 3% systematic error; according to the ASM team this will likely be an underestimate of the error in many cases. The method outlayed above is in principle only applicable if the source spectrum is comparable to that of the Crab. However, since I am only interested in rough estimates my procedure is adequate.

In the spectral analysis the interstellar absorption column, N_H, was fixed at 1.7×10^{21} cm^{-2} (Christian & Swank 1997). Whenever the goodness of fits in the spectral or temporal analyses, expressed as reduced χ^2 ($\chi^2_{\rm red}$) for certain degrees of freedom (dof), exceeded 1, the error bars in the data points were arbitrarily increased so that $\chi^2_{\rm red}=1$. I then determined uncertainties in the fitted parameters using $\Delta\chi^2=1$.

3. Results

By visually inspecting the ASM 1.5–12 keV database of GX 3+1 a single flare was found on 1998 June 9 (MJD 50973). It had a maximum count rate of about 82 cts s^{-1} SSC^{-1}, which was about 5 times brighter than the count rate seen before and after the event (Fig. 1b). It started between UT June 8 22:53:30 and June 9 00:50:40. The decay is exponential-like with a decay time of $\simeq$1.6 hr (1.5–12 keV). About 4.4 hours after the peak of the flare the count rate (27 ± 2 cts s^{-1} SSC^{-1}) was still above the pre-flare persistent level ($\simeq$17 cts s^{-1} SSC^{-1}), suggesting the event lasted even longer. From the end of the last pre-flare measurement and the first measurement at the per-

[2] Note that this matrix is also used by PIMMS (`http://legacy.gsfc.nasa.gov/docs/software/tools/pimms.html`).

sistent count rate after the flare (June 9 15:05:04) I infer an upper limit on the duration of the flare of 16.2 hours.

In Table 1 the fitted exponential decay times of the long flare in the total energy band and the three subbands are listed. They were determined using the flare data plus the persistent data up to a day after the start of the flare. The decay time in the 5–12 keV band is significantly shorter than that in the 3–5 keV band, indicating spectral softening during the decay. This was verified by determining hardness ratios, using the following procedure. I first averaged the count rates in the three energy bands of data within 30 min bins. Then the ratio of the count rates in a hard to low energy band was computed (there are five possible independent combinations with the three available energy bands). I then investigated the flare hardness values during the decay and compared them with those of the persistent emission. It turned out that ratio of the count rates in the 5–12 keV and 1.5–3 keV energy bands gave the best indication for spectral cooling during the day, see Fig. 1c. At flare maximum the source is harder with respect to just before the flare; during the decay of the flare the source softens.

To estimate the observed maximum flux and the fluence of the flare I performed X-ray spectral fits to the ASM data (see Sect. 2). The emission of normal type I bursts can be well described by emission from a black-body (Swank et al. 1977; Lewin et al. 1993). This also holds for the superbursts (e.g. Cornelisse et al. 2000). The flare was divided into three intervals which are indicated by dotted lines in Fig. 1b. The average pre-flare persistent emission between MJD 50971.5 and 50973 was subtracted from the total flare emission per interval. A black-body emission model subjected to interstellar absorption was used; The results of the fits are given in Table 1. Since the peak luminosity is well below the Eddington luminosity (see Sect. 4) the radius of the emission region is expected to be constant during the decay. I, therefore, also fitted the spectra from the three intervals together, coupling the apparent black-body radius, $R_{\rm bb}$, to one value. The results of these fits are also given in Table 1; I get $R_{\rm bb}$=5.4±1.5 km. The values of $R_{\rm bb}$ obtained in the above spectral fits are more or less comparable to those found during the decay of the radius expansion burst seen from GX 3+1 (Kuulkers & van der Klis 2000: ≃7.6 km at 5 kpc). Similar results are derived for e.g. KS 1731−260 (Kuulkers et al. 2001). I, therefore, also performed spectral fits with $R_{\rm bb}$ fixed at 7.6 km, of which the results are also shown in Table 1. Note that some of the values for $\chi^2_{\rm red}$ are unrealistically low; this is most likely due to an overestimate of the errors in the data points by including the rms in the average Crab values. The spectral fits, however, indicate that the black-body temperature, $kT_{\rm bb}$, is in the range 1–2 keV, and decreases, as expected, during the decay of the flare.

To get the values for the observed maximum flux and fluence, the individual dwell net-flare (= total flare minus pre-flare) count rates were converted into fluxes, using the count rates and average fluxes in the three intervals as obtained in the spectral fits with $R_{\rm bb}$ left free. The decay in net-flare flux was fitted with an exponential and assumed it approached zero at infinity. The fluence was calculated by integrating the exponential from the start of the flare up to infinity. I note that this may underestimate the fluence, since the flare probably started somewhat earlier. Extrapolating the fitted exponential backwards in time and assuming the maximum flux can not exceed the Eddington limit (see Sect. 4) an estimate of the upper limit on the fluence, $E_{\rm b,max}$, may be obtained. The results are displayed in Table 1.

Table 1. Flare characteristics

Exponential decay times				
Band	$\tau_{\rm exp}$ [a]	$\chi^2_{\rm red}$/dof		
(keV)	(hr)			
1.5–12	1.6 ± 0.2	2.4/21		
1.5–3	$1.8^{+1.5}_{-0.9}$	0.9/21		
3–5	$2.9^{+1.1}_{-0.7}$	2.3/21		
5–12	1.41 ± 0.15	2.3/21		
X-ray spectral fits: $R_{\rm bb}$ free				
Interval	$F_{\rm bb}$ [b]	$kT_{\rm bb}$ (keV)	$R_{\rm bb}$ [c]	$\chi^2_{\rm red}$/dof
1	3.0 ± 0.4	2.2 ± 0.3	6 ± 1	1.7/1
2	0.9 ± 0.3	2.0 ± 0.6	4 ± 2	0.25/1
3	0.6 ± 0.1	1.2 ± 0.3	8^{+5}_{-3}	0.01/1
X-ray spectral fits: $R_{\rm bb}$ coupled				
Interval	$F_{\rm bb}$ [b]	$kT_{\rm bb}$ (keV)	$R_{\rm bb}$ [c]	$\chi^2_{\rm red}$/dof
1	≃3.0	$2.2^{+0.5}_{-0.3}$	5.4 ± 1.5	0.7/5
2	≃0.8	1.6 ± 0.3	5.4 ± 1.5	0.7/5
3	≃0.6	1.5 ± 0.3	5.4 ± 1.5	0.7/5
X-ray spectral fits: $R_{\rm bb}$ fixed				
Interval	$F_{\rm bb}$ [b]	$kT_{\rm bb}$ (keV)	$R_{\rm bb}$ [c]	$\chi^2_{\rm red}$/dof
1	2.5 ± 0.2	1.80 ± 0.04	7.6	2.5/2
2	0.7 ± 0.1	1.31 ± 0.07	7.6	1.7/2
3	0.6 ± 0.1	1.23 ± 0.08	7.6	0.01/2
Flare parameters				
$F_{\rm bb,max}$ [d]	$E_{\rm b}$ [e]	$E_{\rm b,max}$ [f]	τ (hr) [g]	
3.3 ± 0.6	≃1.7	≃5.3	≃1.5	

[a] Exponential decay time.
[b] Unabsorbed black-body flux (10^{-8} erg cm^{-2} s^{-1}).
[c] Apparent black-body radius at 5 kpc.
[d] Peak unabsorbed black-body flux (10^{-8} erg cm^{-2} s^{-1}).
[e] Fluence in 10^{-4} erg cm^{-2}.
[f] Estimated maximum fluence in 10^{-4} erg cm^{-2}, see text.
[g] $\tau \equiv E_{\rm b}/F_{\rm bb,max}$.

An estimate of the recurrence time of such flares is an important constraint on the physics of the flare. In my case this is very uncertain, given only one observed flare in 5.8 yrs. One could naively deduce that flares happen every 5.8 yrs, but this obviously assumes they occur periodically and that the source was continuously observed in that interval. There are, however, about 15600 dwells of 90 s in that timespan, implying an exposure time of only 16 days; they are also not equally spaced in time and the number of dwells per day varies wildly up to about 140 per day. Another flare could thus have happened during data gaps of longer than the flare duration, whereas one could rule out another flare when there are more than one dwell data point with the source at its persistent count rate in a time span shorter than the flare duration. I used

the observed flare to estimate the total effective exposure time during which only one flare occurred, which may be used as a rough indicator on the recurrence time. The flare profile was characterized by an exponential in the 1.5–12 keV band, as determined by the fit to the decay, with a start point corresponding to the observed peak of $82\,\mathrm{cts\,s^{-1}\,SSC^{-1}}$. A window of 0.2 day was used (approximately the lower limit on the duration of the flare), which was moved throughout all dwell data points. I determined whether or not the flare could fit within the window by determining the $\chi^2_{\rm red}$ between the expected profile and the observed data points (note that I varied the expected persistent count rates and logged the smallest values of $\chi^2_{\rm red}$). Whenever $\chi^2_{\rm red}$ exceeded 2.5 (about the same value as for the exponential fit to the decay light curve), I concluded that within the window no such flare could have occurred; if it was less than 2.5 a flare could have occurred and only the individual dwell durations were taken into account. In this way I estimate a total effective exposure time of about 490 days. Note that this estimate is dependent on the used window length. If I use a window of 0.1 or 0.3 day I derive $\simeq$320 days and $\simeq$600 days, respectively.

4. Discussion

I found an X-ray flare from GX 3+1 in RXTE/ASM data spanning about 6 yrs; the flare had a decay time of 1.6 hr and a duration of longer than 4.4 hr, but shorter than 16.2 hr. During the exponential-like decay the flare spectrum softened. I conclude that the flare has its origin in unstable thermonuclear burning. The total fluence of the event is between about 5×10^{41} erg and 2×10^{42} erg for a distance of 5 kpc. The maximum net-burst flux reached during a normal type I X-ray burst seen by Kuulkers & van der Klis (2000) was $6.9\times10^{-8}\,\mathrm{erg\,cm^{-2}\,s^{-1}}$. Since this burst was a radius-expansion event the corresponding luminosity at the neutron star surface reached the Eddington limit. The flare, therefore, had an observed maximum of about 0.5 times the Eddington value (but note that the actual peak of the flare was missed). The persistent ASM count rate before and after the flare was similar to that observed around the radius expansion burst, indicating the persistent flux near the X-ray flare was about 0.2 times the Eddington value.

The long X-ray flare bears all the characteristics of the superbursts discovered recently in five other X-ray burst sources: 4U 1735−44, Ser X-1, 4U 1636−53, 4U 1820−30 and KS 1731−260 (Cornelisse et al. 2000, 2001; Wijnands 2001; Strohmayer & Brown 2001; Kuulkers et al. 2001). They have been shown to be thermonuclear events on the surfaces of neutron stars, in which carbon (Cumming & Bildsten 2001; Strohmayer & Brown 2001) or electron capture (Kuulkers et al. 2001) plays the dominant role.

Assuming the persistent luminosity is a direct measure of the mass accretion rate, $\dot{M}$, onto the neutron star, one would infer $\dot{M}\simeq2\times10^{17}\,\mathrm{g\,s^{-1}}$ in GX 3+1 just before the superburst. But since the persistent luminosity is variable by a factor of $\simeq$2 and at the time of the superburst it was at a minimum as seen by the ASM in $\simeq$6 yrs, I assume an average $\dot{M}$ of $\simeq3\times10^{17}\,\mathrm{g\,s^{-1}}$. If the ignition of the superburst occurs in a carbon-rich layer, recurrence times of $\simeq$13 yrs are then expected, unless the ignition is prematurely triggered (Strohmayer & Brown 2001). Note that this case is applicable to a neutron star accreting pure helium, such as 4U 1820−30. Of the other systems, only 4U 1735−44 and 4U 1636−53 are known to have hydrogen-rich donors (Augusteijn et al. 1998); this is not as yet clear for GX 3+1. For hydrogen/helium accreting neutron stars it has been shown that carbon may ignite earlier when in an ocean of heavy elements, leading to a smaller recurrence time of $\simeq$2 yrs at the average $\dot{M}$ (Cumming & Bildsten 2001). If, on the other hand, the superbursts are due to unstable electron capture by protons with subsequent capture of the resulting neutrons by heavy nuclei, then recurrence times of less than 0.5 yr are expected (Kuulkers et al. 2001). The expected recurrence times in the latter two cases are more or less compatible with seeing one superburst from GX 3+1 in a total effective exposure time of about 1 to 1.5 yrs, as well as seeing two such events 4.7 yrs apart from 4U 1636−53 (Wijnands 2001). Effective exposure times can in principle be determined for the other superburst sources, using RXTE/ASM data together with data from other instruments (e.g. BeppoSAX/WFCs); however, this is outside the scope of this paper. Longer and more frequent monitoring of these sources will enable one to discriminate the origin of the superbursts.

Acknowledgements. I thank Al Levine for providing the ASM on-source effective area matrix and discussions related to it, Jean in 't Zand for comments on an earlier draft, Andrew Cumming and Lars Bildsten for a discussion on the recurrence times, and the referee for useful comments. I acknowledge the use of ASM data products provided by the ASM/RXTE team (`http://xte.mit.edu`; `http://heasarc.gsfc.nasa.gov/docs/xte/asm_products.html`).

References

Augusteijn, T., van der Hooft, F., de Jong, J.A., van Kerkwijk, M.H., & van Paradijs, J. 1998, A&A, 332, 561
Christian, D., & Swank, J.H. 1997, ApJS, 197, 177
Cornelisse, R., Heise, J., Kuulkers, E., Verbunt, F., & in 't Zand, J.J.M. 2000, A&A, 357, L21
Cornelisse, R., Kuulkers, E., in 't Zand, J.J.M., Verbunt, F., & Heise, J. 2001, A&A, in press [astro-ph/0111263]
Cumming, A., & Bildsten, L. 2001, ApJ, 559, L127
Kuulkers, E. 2001, ATel #68
Kuulkers, E., & van der Klis, M. 2000, A&A, 356, L45
Kuulkers, E., in 't Zand, J.J.M., van Kerkwijk, M.H., et al. 2001, A&A, in press [astro-ph/0111261]
Levine, A.M., Bradt, H., Cui, W., et al. 1996, ApJ, 469, L33
Lewin, W.H.G., van Paradijs, J., & Taam, R.E. 1993, Space Sci. Rev., 62, 223
Makishima, K., Mitsuda, K., Inoue, H., et al., 1983, ApJ, 267, 310
Schattenburg, M.L., & Canizares, C.R. 1986, ApJ, 301, 759
Strohmayer, T.E., & Brown, E.F. 2001, ApJ, in press [astro-ph/0108420]

Swank, J.H., Becker, R.H., Boldt, E.A., Holt, S.S., Pravdo, S.H., & Serlemitsos, P.J. 1977, ApJ, 212, L73
Wijnands, R. 2001, ApJ, 554, L59